Hydrodynamic Forces on Flexible Offshore Structures[a]

By Enrique J. Laya,[1] Jerome J. Connor,[2] M. ASCE, and S. Shyam Sunder,[3] A. M. ASCE

Abstract: The extension of Morison's equation to allow for structural motion in predicting the hydrodynamic force on offshore steel jacket platforms may be based on two different hypotheses: (1) The relative velocity model which replaces the fluid velocity by the relative velocity between the fluid and the structure; and (2) the independent flow fields model which considers the flow to be a superposition of two unrelated flows, one due to the wave-current action on a rigid cylinder, and the other due to the structural motion in still water. An iterative computational procedure that combines time domain and frequency domain analysis techniques is developed to solve the nonlinear governing equations for both models. Comparison studies are carried out for seastates ranging from the drag dominant through the inertia dominant regimes. Results indicate that the independent flow fields model always predicts a higher structural velocity response, the difference increasing with wave height. There is negligible difference for the inertia dominant range. At intermediate seastates, which are of primary concern for fatigue analysis, the relative velocity model appears to overestimate the damping. Consequently, its use in fatigue life prediction may be questioned. For typical offshore platforms, the applicability of the independent flow fields model diminishes as the seastate approaches extreme values.

Introduction

The dynamic response of steel jacket offshore platforms under wave excitation may be significantly influenced by the total amount of damping present in the system. One of several sources of damping, and of particular importance in estimating the response of deep water structures, is the hydrodynamic drag damping arising from fluid-structure interaction effects. The fundamental period of vibration of such deep water platforms is close to the range of dominant periods associated with wave loading and, consequently, their dynamic response tends to be "damping controlled." An accurate estimation of damping is also crucial for the prediction of structural joint fatigue life, an important design consideration for these structures.

Most studies use Morison's equation (17) for predicting the in-line forces exerted by viscous oscillatory flows on stationary slender vertical cylinders:

$$f = \frac{1}{2}\rho C_D D v|v| + \rho \frac{\Pi D^2}{4} C_M \dot{v} \quad \ldots\ldots (1)$$

[a]Presented at the June, 1981, Joint ASME/ASCE Mechanics Conference held in Boulder, Colo.

[1]Research Engr., INTEVEP, S.A., Caracas, Venezuela.

[2]Prof. of Civ. Engrg., Massachusetts Inst. of Technology, Cambridge, Mass. 02139.

[3]Asst. Prof. of Civ. Engrg., Massachusetts Inst. of Technology, Cambridge, Mass. 02139.

Note.—Discussion open until August 1, 1984. To extend the closing date one month, a written request must be filed with the ASCE Manager of Technical and Professional Publications. The manuscript for this paper was submitted for review and possible publication on September 22, 1982. This paper is part of the *Journal of Engineering Mechanics*, Vol. 110, No. 3, March, 1984. ©ASCE, ISSN 0733-9399/84/0003-0433/$01.00. Paper No. 18624.

in which f = the in-line force per unit length; ρ = the water density; D = the cylinder diameter; v and $\dot{v}$ = the water particle velocity and acceleration, respectively; and C_D, C_M are the hydrodynamic drag and inertia force coefficients. Hogben, et al. (8) provide a comprehensive review of published data on C_D and C_M.

Keulegan and Carpenter in their classic 1958 paper (10) postulated that the harmonic fluid forces on a cylinder (and consequently both C_D and C_M) are, in general, functions of Reynolds number, R, and a nondimensional "period" parameter proportional to the ratio of drag and inertia forces, K-C, now called the Keulegan-Carpenter number. For a two-dimensional oscillatory flow with velocity amplitude V_o and period T, the Reynolds number and Keulegan-Carpenter number are defined as

$$\mathrm{R} = \frac{V_o D}{\nu} \quad \text{K-C} = \frac{V_o T}{D} \qquad (2)$$

in which ν = the fluid kinematic viscosity. The Keulegan-Carpenter number is proportional to the ratio of the distance travelled by the water particle each half cycle to the cylinder diameter and can be interpreted as a measure of the unsteadiness of the flow. Note that in oscillatory flows, flow reversal occurs every half cycle. At high values of K-C, i.e., $\gtrsim$25, the velocity of the flow varies slowly compared to the wake development time, and the flow can be considered as quasisteady. In this situation, the drag force dominates over the inertia force and the drag coefficient tends to its value for steady flow with increasing K-C. At low values of K-C, i.e., $\lesssim$5, the drag force term tends to zero and the inertia component tends to dominate. The least well understood wave loading regime, and therefore, the one with the least accurate description, is the regime with $5 \lesssim$ K-C $\lesssim 25$, in which both drag and inertia forces are important.

Many studies have been directed at establishing the dependence of C_D and C_M on R and K-C. For example, while Keulegan and Carpenter's experiments confirmed the functional dependence of time-averaged values of C_D and C_M on K-C, they were unable to establish a correlation between the coefficients and Reynolds number. The dependence of the force coefficients on both R and K-C was shown for the first time by Sarpkaya (20,21) through a reanalysis of the data given by Keulegan and Carpenter and an extensive experimental investigation with two-dimensional simple harmonic oscillatory flow past a cylinder in a U-shaped water tunnel. Sarpkaya's work also established the dependence of the force coefficient for rough cylinders on the relative roughness of the cylinders, k/D. These coefficients differ significantly from those corresponding to a smooth cylinder. The present study utilizes Sarpkaya's results for rough cylinders as presented in Ref. 23 and the procedure outlined in Ref. 24 to estimate the hydrodynamic loads.

Fluid-structure interaction needs to be considered when the level of structural motion is not negligible. Several investigators (2,12,14) have attempted to take into account the effect of structural flexibility in force evaluations by modifying the original Morison equation to include interactive terms that involve both the fluid and the structural velocities and accelerations. In the process it is assumed that the interaction be-

tween the incident fluid flow and the resulting structural motion is linear, i.e., the resulting flow field kinematics are equal to the algebraic difference between the kinematics of the incident fluid flow and the resulting kinematics of the structure. The validity of this assumption, which determines the level of hydrodynamic drag damping, is questionable.

This paper compares the results from the existing "relative velocity" model with those from another model, the independent flow fields model, originally postulated and investigated for steady flow conditions by Moe and Verley (15,16). The regions of validity of the two force formulations are qualitatively established. An iterative computational procedure that combines both time domain and frequency domain analysis techniques is developed to solve the nonlinear governing equations for both models. Comparison studies for seastates ranging from the drag dominant through the inertia dominant regimes indicate that the independent flow fields model always predicts a higher structural velocity response, the difference increasing with wave height. There is negligible difference for the inertia dominant range. At intermediate seastates, which are of primary concern for fatigue analysis, the relative velocity model appears to overestimate the damping. Consequently, its use in fatigue life prediction may be questioned. For typical offshore platforms, the applicability of the independent flow fields model diminishes as the seastate approaches extreme values.

Hydrodynamic Force Modeling

Relative Velocity Model.—The modified form of the Morison equation under the relative velocity assumption is given by

$$f = \frac{1}{2}\rho C_D D(v - \dot{u})\,|v - \dot{u}| + \rho\frac{\Pi D^2}{4}[C_M\dot{v} - (C_M - 1)\ddot{u}] \quad \ldots\ldots\ldots\ldots (3)$$

in which $\dot{u}$ and $\ddot{u}$ = the cylinder velocity and acceleration, respectively. The two basic differences between Eqs. 1 and 3 are: (1) The drag force has been assumed to be proportional to the square of the relative velocity; and (2) the inertia force contains an added mass term proportional to the cylinder acceleration. The hydrodynamic drag and inertia force coefficients may be evaluated with a "relative velocity definition" of R and K-C:

$$R = \frac{\dot{r}_o D}{\nu} \quad K\text{-}C = \frac{\dot{r}_o T_{\dot{r}}}{D} \quad \ldots\ldots\ldots\ldots\ldots\ldots\ldots\ldots\ldots\ldots\ldots\ldots\ldots\ldots (4)$$

in which $\dot{r}_o$ = the amplitude of the relative velocity, $\dot{r} = v - \dot{u}$; and $T_{\dot{r}}$ = the period of $\dot{r}$. Note that even if v and $\dot{u}$ are harmonic functions, $\dot{r}$ need not be sinusoidal.

The relative velocity form of Morison's equation is rather heuristic even though it may seem to be an obvious extension of the original form which in itself has several uncertainties. Eq. 3 should be interpreted as an entirely new empirical formula that needs to be verified experimentally. Furthermore, the use of Eq. 4 in evaluating C_M and C_D is not strictly justified. However, it is possible to gain some insight as to the appropriateness of the relative velocity assumption by studying (qualitatively)

the different behavioral modes that may be observed when an external oscillatory flow is directed at an oscillating cylinder.

An alternate interpretation is first established for the Keulegan-Carpenter number in terms of the time required for a wake to develop around a cylinder which starting from an initial at rest position is translated through calm water. An appropriate measure for this is the vortex shedding period, T_s, given by

$$T_s = \left(\frac{1}{S}\right)\left(\frac{D}{v}\right) \quad \text{(5)}$$

in which S = the Strouhal number which depends on R. In harmonically oscillating flow past a fixed circular cylinder, the wake development time may still be considered proportional to T_s, and for simplicity to D/V_o if Reynolds number is a constant. However, the presence of flow reversals can inhibit the formation of the wake. A measure of the time available for a wake to develop is the period of oscillation, T. Thus, it is possible to interpret the Keulegan-Carpenter number defined in Eq. 2 as the ratio

$$\text{K-C} \propto \frac{\text{Time available for a wake to form}}{\text{Time required for a wake to form}} \quad \text{(6)}$$

If cylinder motion is prescribed in terms of an amplitude U_o and period T_o, two additional parameters, the reduced velocity, V_R, and the dimensionless amplitude measure, $\hat{U}$, are introduced:

$$V_R = \frac{V_o T_o}{D} \quad \text{(7a)}$$

and

$$\hat{U} = \frac{U_o}{D} \quad \text{(7b)}$$

The reduced velocity may be interpreted in a way similar to the Keulegan-Carpenter number. Here the time available for a wake to form is the period of oscillation of the cylinder.

A full description of the problem in terms of all five parameters is not available at the present time. However, experimental results have been obtained for the case of a stationary cylinder in oscillatory flow and for an oscillating cylinder in steady current. Much of this work has been reviewed in a recent book by Sarpkaya and Isaacson (22). Assuming some typical orders of magnitude for R ($10^5 - 10^6$) and k/D (0.01, rough cylinder), it is possible to pursue the behavioral assessment by varying K-C, V_R and $\hat{U}$.

The situation where K-C and V_R are both very high and $\hat{U}$ is extremely high typically occurs for a compliant tower or a tension leg platform under moderate to extreme seastate conditions. For conventional jacket type structures in shallow to intermediate water depths, K-C and V_R are usually high under design seastates although $\hat{U}$ is small. In both these cases it is possible to argue that the drag force will result from the superposition of two "dependent," quasi-steady flow fields; one due to an almost "steady" flow past the cylinder at rest and the other due to the slow motion of the cylinder through relatively "calm" water. Here the

in-line drag force per unit length, after accounting for the sense of the force, would be given by the first term in Eq. 3. It is important to recognize that the relative velocity form of the drag term does apply when there exists a well defined wake and the flow is quasi-steady.

Independent Flow Fields Model.—The case of high K-C and small V_R corresponds to a resonating and/or a superharmonically resonating drag dominated structure, i.e., a rapidly vibrating cylinder in a relatively slowly oscillating external flow. Here any vortex initiation is virtually eliminated by the cylinder due to its high rate of vibration. Under these conditions, the water particles near the cylinder's field of influence follow a widly disorganized and unsteady flow pattern. The use of a relative velocity formulation in this case would be highly suspect. This finding would also hold for the case of a low K-C and high V_R, i.e., a low frequency cylinder oscillation in a high frequency flow oscillation. Fig. 1 summarizes this qualitative discussion. The numerical limits suggested in the figure are based on Moe and Verley's experimental work (15,16) for a steady current past an oscillating cylinder. They found that $V_R \simeq$ 10–15 as the limiting value for which the relative velocity formulation gives reliable results. This range is suggested here to be the limit boundary for V_R when K-C $\rightarrow \infty$ and for K-C where $V_R \rightarrow \infty$. It can be seen from Fig. 1 that the relative velocity assumption may not be applicable over a wide range of intermediate values for K-C and V_R when higher rates of oscillation in both the external flow and the cylinder are involved.

A different form of the drag force term has been proposed by Moe and Verley (15,16) for conditions under which the relative velocity formulation is inappropriate. Their formulation, valid for cylinder oscillation in steady flow and tested with experiments at very low Reynolds numbers, is based on the superposition of two "independent" flow fields, a far field which is unaffected by the cylinder motion and a near field resulting from the cylinder motion. Extending this concept to the case of an oscillatory external flow yields the following drag force term:

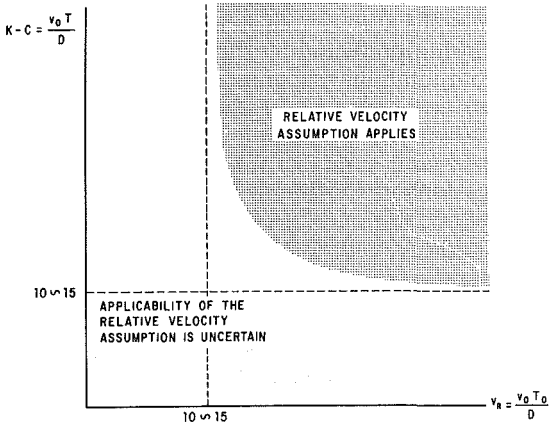

FIG. 1.—Qualitative Ranges for Applicability of Alternate Hydrodynamic Force Formulations

$$f_D = \frac{1}{2}\rho C_{Dv} D v|v| - \frac{1}{2}\rho C_{D\dot{u}} D\dot{u}|\dot{u}| \quad \ldots\ldots\ldots\ldots\ldots\ldots\ldots\ldots\ldots\ldots \quad (8)$$

in which C_{Dv} = the oscillatory drag force coefficient on a stationary cylinder; and $C_{D\dot{u}}$ is the oscillatory drag force coefficient for a cylinder vibrating in still water. The total hydrodynamic force, after incorporating the independent flow fields assumption into the inertia force term, can be expressed as

$$f = \frac{1}{2}\rho D[C_{Dv} v|v| - C_{D\dot{u}} \dot{u}|\dot{u}|] + \rho \frac{\Pi D^2}{4}[C_{Mv}\dot{v} - (C_{M\dot{u}} - 1)\ddot{u}] \quad \ldots\ldots\ldots \quad (9)$$

where the hydrodynamic force coefficients are proposed to be evaluated by hypothesizing that

$$C_{Dv},\ C_{Mv} = f\left(\mathrm{R}_F = \frac{V_o D}{\nu},\quad \text{K-C}_F = \frac{V_o T}{D},\quad \frac{k}{D}\right) \quad \ldots\ldots\ldots\ldots\ldots\ldots \quad (10a)$$

$$C_{D\dot{u}},\ C_{M\dot{u}} = f\left(\mathrm{R}_N = \frac{\dot{U}_o D}{\nu},\quad \text{K-C}_N = \frac{\dot{U}_o T_o}{D},\quad \frac{k}{D}\right) \quad \ldots\ldots\ldots\ldots\ldots\ldots \quad (10b)$$

The suffix F indicates far field while the suffix N indicates near field.

Based on a comparison of the two force formulations given in Eqs. 3 and 9, the observations can be made: (1) The independent flow fields model is expected to yield a lower hydrodynamic drag damping value and consequently produce higher response amplitudes. Note that under typical conditions $|\dot{u}| << |v|$ and therefore the term $1/2\rho DC_{D\dot{u}}\dot{u}|\dot{u}|$ will be smaller than $1/2\rho DC_D|v - \dot{u}|\dot{u}$; and (2) the independent flow fields model may yield a higher added mass term since $C_{M\dot{u}}$ may be larger than C_M. However, for typical offshore platforms that have a very large nonimmersed mass, this effect may be unimportant.

Computational Scheme

In order to assess the differences in structural response and hydrodynamic drag damping predicted by the two force formulations, a simple but accurate computational scheme capable of handling the full nonlinear forcing term is developed. Numerical implementation and convergence considerations for the solution procedures are also discussed in what follows.

Solution of Equations of Motion.—The basic equations of motion for predicting the dynamic response of offshore platforms may be expressed as

$$(\underline{\mathbf{M}} + \underline{M}_a)\ddot{\underline{\mathbf{U}}}(t) + \underline{\mathbf{C}}\dot{\underline{\mathbf{U}}}(t) + \underline{\mathbf{K}}\underline{\mathbf{U}}(t) = \underline{\mathbf{F}}(\dot{\underline{\mathbf{U}}}, t) \quad \ldots\ldots\ldots\ldots\ldots\ldots\ldots \quad (11)$$

in which $\underline{\mathbf{M}}$, $\underline{\mathbf{C}}$ and $\underline{\mathbf{K}}$ = the mass, fluid and foundation radiation damping, and stiffness matrices, respectively, for the offshore structure system. $\underline{M}_a$ represents the added mass term in either Eq. 3 or 9. The vector $\underline{\mathbf{F}}(\dot{\underline{\mathbf{U}}}, t)$ represents either Eq. 3 or Eq. 9 without the added mass term. The actual distributed loads are modeled as point loads at the nodes of the discretized offshore system. Structural damping is modeled in terms

of a linear hysteretic damping coefficient, D_S, that is proportional to the stiffness matrix, $\underline{\mathbf{K}}$:

$$\text{Im}[\underline{\mathbf{K}}] = 2D_S \,\text{Real}\,[\underline{\mathbf{K}}] \quad \ldots\ldots (12)$$

in which Im[ ] denotes the "imaginary part of."

A major problem in solving Eq. 11 is the treatment of the nonlinear response dependent form of the drag force in $\underline{\mathbf{F}}(\dot{\underline{\mathbf{U}}}, t)$. Nondeterministic frequency domain approaches to solving these equations generally assume the excitation and the response to be Gaussian random processes and linearize the drag force term (1,3,7,12,25). This assumption is reasonable only when the drag force term is smaller than the inertia force term. Dunwoody (5) has investigated the use of a third order expansion for the zero mean random wave case. Unfortunately, none of these methods treat the drag term in its full nonlinear form. On the other hand, deterministic time-domain approaches, although capable of handling nonlinearities, have problems with the isolation of starting transients in the response record. Since the seastate is modeled as a stationary random process, interest typically is in obtaining the steady state rather then the transient response of the platform. Moreover, specification of the time-dependent hydrodynamic force coefficients that depend on prior knowledge of the response is not possible without iterating on the entire nonlinear solution.

A procedure which generates the full nonlinear solution to the equations of motion and avoids the problem of starting transients is applied here. The approach is based on a modification of the deterministic, iterative frequency domain method of Fish and Rainey (6). The modification involves using a second order truncation of the Taylor series for the force about a reference response function rather than the first order truncation used in Ref. 6. Inclusion of the higher order derivative accelerates convergence. While the solution procedure yields only a deterministic response record, it is possible to derive the response spectral density function with high resolution spectral estimators such as the maximum entropy (MEM) spectral estimator (4) that require relatively short response time-histories. Transients in the response record are eliminated by implementing a circular convolution (18) using the Discrete Fourier Transform (DFT). The Fast Fourier Transform (FFT) is a high speed algorithm for computing the DFT. Circular convolution is valid when the segment of the stationary random force process is considered to be periodic with period equal to the duration of the segment. This is a reasonable assumption for the force time-history.

The hydrodynamic force coefficients are updated in each iteration cycle. Since the wave excitation is expressed as a spectrum, a procedure for chosing the coefficients needs to be established. Assuming the root-mean-square velocity and the average zero-crossing period as characteristic values, the time-averaged hydrodynamic coefficients may be evaluated with the procedure suggested by Angelides and Connor (1).

$$C_D, C_M = f\left(\mathrm{R} = \frac{\sigma_{\dot{r}} D}{\nu},\quad \text{K-C} = \frac{\sigma_{\dot{r}} T_{\dot{r}}}{D},\quad \frac{k}{D}\right) \quad \ldots\ldots (13a)$$

$$C_{Dv}, C_{Mv} = f\left(\mathrm{R}_F = \frac{\sigma_v D}{\nu_D},\quad \text{K-C}_F = \frac{\sigma_v T_v}{D},\quad \frac{k}{D}\right) \quad \ldots\ldots (13b)$$

$$C_{D\dot{u}}, D_{M\dot{u}} = f\left(R_N = \frac{\sigma_{\dot{u}} D}{\nu}, \quad K\text{-}C_N = \frac{\sigma_{\dot{u}} T_{\dot{u}}}{D}, \quad \frac{k}{D}\right) \quad \text{..... (13c)}$$

in which σ_r is r.m.s. value of $(v - \dot{u})$, T_r is the average zero-crossing period of $(v - \dot{u})$, and similarly for the other terms. These hydrodynamic coefficients vary with depth below still water level.

Numerical Implementation.—The numerical solution of the equations of motion requires the use of finite duration time-histories for both load and response, and also operating in discrete time and frequency domains. The sampling period or time increment is chosen such that aliasing distortions are avoided in the numerical solution. The actual frequency content of the forcing function depends upon the wave surface elevation spectral density function. Primarily due to the nonlinear nature of the drag force term, the energy content at the higher frequency end of the force spectrum is greater than that in the wave surface elevation spectrum. Also, a series of peaks are present at $3\Omega_p$, $5\Omega_p$, etc., where Ω_p is the peak frequency of the wave spectrum, due to the drag force term. The presence of a current would introduce additional peaks at even multiples of Ω_p. The choice of sampling period must also ensure that the structural natural frequencies of interest are adequately resolved. Additionally, if the sampling period is too large, the series of cusps that may be present in the response velocity time-history could be improperly resolved or lost. The presence of these cusps has been shown by Mes (13) and is discussed in Ref. 11.

Convergence Considerations.—In order to assess the accuracy of the iterative solution, both extreme and global convergence measures, the peak difference in two consecutive response velocity time-histories and the corresponding r.m.s. values, respectively, are considered. The peak differences are checked only when the solution is approaching convergence.

Convergence can be improved by using an initial hydrodynamic drag damping term in the equations of motion. The idea is to precondition the initial response estimate which would otherwise consider no hydrodynamic drag damping. As suggested by Fish and Rainey (6), a hydrodynamic drag damping matrix resulting from a linear, Gaussian expansion of the drag force would yield a reasonable starting estimate. However, the use of artificial damping as a fraction, α, of the linearized hydrodynamic drag damping per unit length of $1/2\ \rho D C_{Dv} \sqrt{8/\Pi}\ \sigma_v$ is preferred. Values of α close to one are reasonable for the relative velocity model while lower values are needed for the independent flow fields model which predicts lower levels of damping.

Sensitivity Studies

The numerical simulations carried out in this investigation are directed at assessing the sensitivity of an offshore platform response to the two hydrodynamic force formulations. Since interpretation of the results from a complete, multi-member offshore platform would be complex, attention is restricted to a single vertical pile structure with diameter comparable to that of a typical platform member and fundamental natural frequency that can easily be adjusted. Properties of the pile used in the

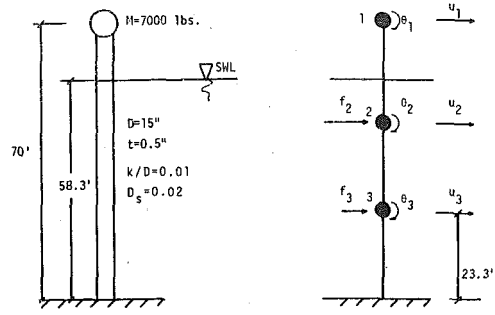

FIG. 2.—Single Vertical Pile Structure for Sensitivity Studies

sensitivity studies, with a fundamental period of approximately three seconds, may be found in Fig. 2.

Employing the two-parameter Modified Pierson-Moskowitz wave surface elevation spectral density function (19), a range of one-dimensional random seastates representing the inertia dominant through the drag dominant regimes is applied to the structure. Deterministic surface elevation time-histories are generated by combining sinusoids with different amplitudes derived from the wave spectrum and phase angles uniformly distributed between zero and 2II. Applying linear wave theory, horizontal fluid particle velocities and accelerations induced by the irregular wave are determined by summing all the component frequency velocities and accelerations.

Sensitivity studies are carried out on the vertical pile structure of Fig. 2 for five different seastates. The root-mean-square top node velocity response for the two force models are plotted as a function of the significant wave height, H_s, in Fig. 3. Formulation I refers to the relative velocity model and Formulation II to the independent flow fields model. The curves show that the relative velocity formulations predicts significantly lower responses than the independent flow fields formulation as H_s increases, and the drag force becomes more dominant. Formulation I predicts large damping values as H_s increases because of the corresponding increase in relative velocities. The drag damping in Formula-

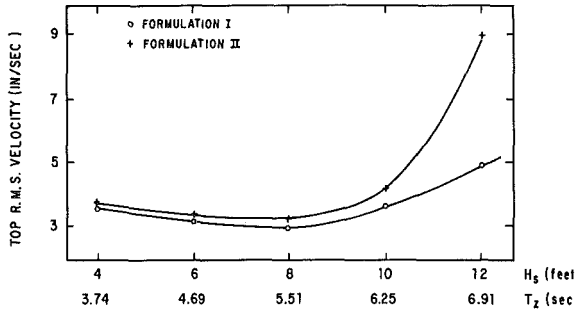

FIG. 3.—Response Sensitivity to Alternate Force Formulations

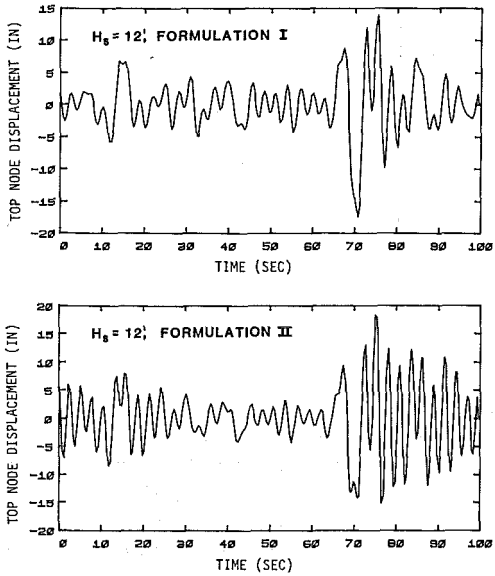

FIG. 4.—Converged Top Node Displacements for Alternate Force Formulations

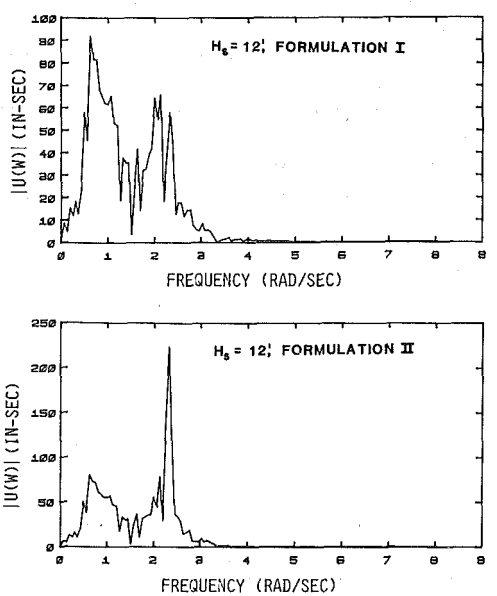

FIG. 5.—Fourier Magnitude Transforms of Converged Top Node Displacements for Alternate Force Formulations (H_s = 12 ft)

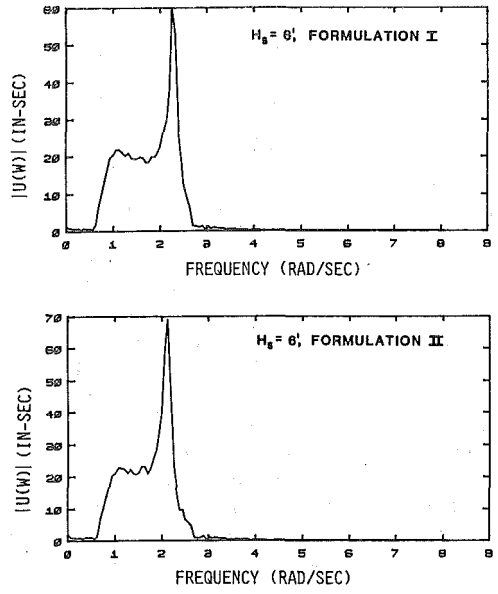

FIG. 6.—Fourier Magnitude Transforms of Converged Top Node Displacements for Alternate Force Formulations (H_s = 6 ft)

tion II arises from the term associated with the structural velocity which in general tends to be much smaller than the fluid velocity. Consequently, the independent flow fields model predicts a lower damping than the relative velocity model. This explains the differences in response as H_s increases. Even though there is dynamic amplification as the average zero-crossing period, T_z, approaches the natural period of

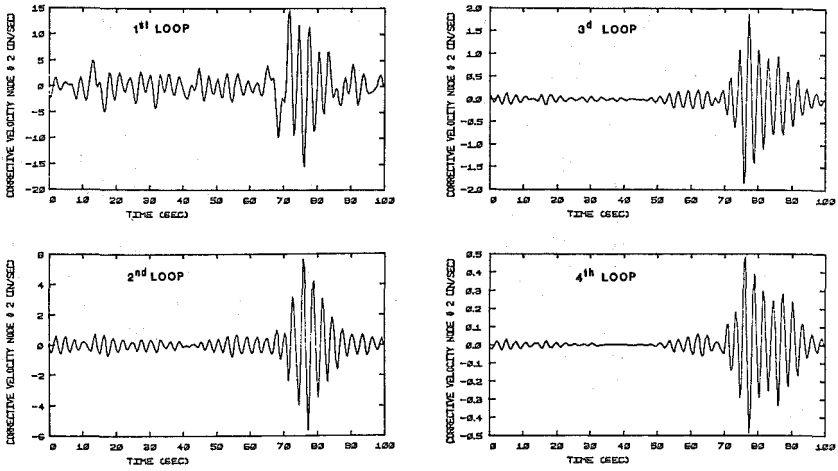

FIG. 7.—Convergence of Corrective Velocity

TABLE 1.—Percentage of Converged Response for Different Fractions of Artificial Damping

Cycle (1)	Formulation I		Formulation II	
	$\alpha = 0.4$ (2)	$\alpha = 1.6$ (3)	$\alpha = 0.05$ (4)	$\alpha = 1.0$ (5)
1	136.97	96.99	95.83	57.10
2	108.40	99.29	100.60	77.34
3	104.13	99.45	99.97	88.30
4	102.00	99.80	99.99	94.80

the pile in the low H_s region, the lack of hydrodynamic drag damping here results in similar responses being predicted by the two models. However, this finding should not be taken too literally since no allowance has been made for radiation damping which is probably more important than drag damping in this region.

The converged top node displacements for the two formulations, and a seastate defined by $H_s = 12$ ft and $T_z = 6.91$ sec, is shown in Fig. 4. Although peak displacements are not significantly different, the frequency content is significantly different for the two signals. This is amply supported by the Fourier magnitude transforms of these signals shown in Fig. 5. As would be expected the response obtained with Formulation II is highly resonant. A different behavior is observed for low significant wave heights. Fig. 6 shows the Fourier magnitude transforms of top node displacements for $H_s = 6$ ft, $T_z = 4.69$ sec. The difference in responses for the two formulations is negligible. As already discussed, dynamic effects are important for the low seastate considered here.

Convergence of the iterative process can be assessed by comparing the corrective velocity at each iteration. The difference in consecutive structural response velocities for the four iterations, made with Formulation I and a seastate defined by $H_s = 12$ ft, at the second node in Fig. 2 are shown in Fig. 7. Convergence over the duration of the signal is uneven due to the presence of a "beat" in the force signal towards the end of the record. As convergence is obtained, the smoother part of the corrective term is zeroed out while the magnitude of the beat pattern is significantly reduced. The occurrence of the beat pattern may be explained in terms of the phase distortions introduced by differences in hydrodynamic drag damping during convergence. Experience with other cases not presented here indicates that the convergence rate increases as the structure becomes stiffer.

Table 1 shows the effect of the artificial damping fraction, α, on convergence for the 12 foot significant wave height case. The table lists the percentages of convergence for the r.m.s. top node displacement response. These results show that convergence can be improved with an appropriate choice of α. For the case under consideration, $\alpha = 1.6$ is preferable for Formulation I while $\alpha = 0.05$ is preferable for Formulation II.

Conclusions

The main objective of this study has been to investigate the sensitivity

of the structural response to two different models for simulating fluid-structure interaction, the relative velocity model and the independent flow fields model. The second approach, originally proposed for a steady current acting on an oscillating cylinder, has been extended to the case of an irregular wave acting on an oscillating structure. An iterative frequency domain deterministic method has been developed to allow for the nonlinear form of the force models and solve the resulting equations of motion for a simplified offshore jacket element consisting of a single vertical pile.

Simulation studies carried out for a pile structure with a fundamental period of three seconds and a range of seastates resulted in the following specific conclusions:

1. The independent flow fields model predicts a lower hydrodynamic drag damping than the relative velocity model. The difference in damping values increases with the severity of the seastate.
2. At low seastates where the drag force and consequently the hydrodynamic drag damping are negligible, the results for the peak and r.m.s. structural velocity responses are in close agreement for the two models.
3. The relative velocity model is more appropriate for structural members associated with high reduced velocities and Keulegan-Carpenter numbers, while the independent flow fields model could be more appropriate in some of the other cases. It might therefore be more realistic to apply the two models selectively over regions (i.e., members) of an offshore platform where they apply.
4. Fatigue damage for a typical deep water platform is a maximum in the low to intermediate seastate range (9). The applicability of the two force formulations in the intermediate seastate range where they predict significantly different responses needs to be established.

The results presented in this paper are based on approximate models and therefore need to be interpreted carefully. For example, both formulations neglect vortex shedding effects which could be important for the flow conditions associated with the seastates considered here. Furthermore, the conclusions depend on the intuitive, yet speculative, generalizations of the original Morison's equation. It is of crucial importance to verify experimentally the form and applicability of the two force models, particularly at the intermediate to extreme seastate range, before they can be recommended confidently for use in practical applications.

Acknowledgments

The Fundación Gran Mariscal de Ayacucho funded the first writer's studies at M.I.T. This research was supported by INTEVEP, S.A. We are most appreciative of their support. Technical comments from Professor Sarpkaya and Professor Paidoussis have been valuable.

Appendix I.—References

1. Angelides, D. C., and Connor, J. J., "Response of Fixed Offshore Structures

in Random Sea," *Journal of Earthquake Engineering and Structural Dynamics*, Vol. 8, Dec., 1980, pp. 503–526.
2. Berge, B., and Penzien, J., "Three-Dimensional Stochastic Response of Offshore Towers to Wave Forces," *Proceedings of the Offshore Technology Conference*, Paper No. 2050, 1974.
3. Borgman, L. E., "Ocean Wave Simulation for Engineering Design," *Journal of Waterways and Harbors Division*, ASCE, Vol. 95, No. WW4, Nov., 1969, pp. 557–583.
4. Burg, J. P., "Maximum Entropy Spectral Analysis," thesis presented to Stanford University, at Palo Alto, Calif., in 1975, in partial fulfillment of the requirements for the degree of Doctor of Philosophy.
5. Dunwoody, A. B., "The Role of Separated Flow in the Prediction of the Dynamic Response of Offshore Structures to Random Waves," thesis presented to the Massachusetts Institute of Technology, at Cambridge, Mass., in 1980, in partial fulfillment of the requirements for the degree of Doctor of Philosophy.
6. Fish, P. R., and Rainey, R. C. T., "The Importance of Structural Motion in the Calculation of Wave Loads on an Offshore Structure," *Proceedings of the Second International Conference on the Behavior of Offshore Structures*, Vol. 2, Paper No. 50, Aug., 1979, pp. 43–60.
7. Gudmestad, O. T., and Connor, J. J., "Linearization Methods and the Influence of Current on the Nonlinear Drag Hydrodynamic Force," *Journal of Applied Ocean Research*, Vol. 5, No. 4, 1983, pp. 184–194.
8. Hogben, N., Miller, B. L., Searle, J. W., and Ward, G., "Estimation of Fluid Loading on Offshore Structures," *Proceedings of the Institution of Civil Engineers*, Part 2, 63, Sept., 1977, pp. 515–562.
9. Kawamoto, J., Shyam Sunder, S., and Connor, J. J., "An Assessment of Uncertainties in Fatigue Analysis of Steel Jacket Offshore Platforms," *Journal of Applied Ocean Research*, Vol. 4, No. 1, 1982, pp. 9–16.
10. Keulegan, G. H., and Carpenter, L. H., "Forces on Cylinders and Plates in an Oscillating Fluid," *Journal of Research of the National Bureau of Standards (United States)*, Vol. 60, No. 5, May, 1958, pp. 423–440.
11. Laya, E. J., "Effect of Structural Motion on the Hydrodynamic Forcing of Offshore Steel Structures," thesis presented to the Massachusetts Institute of Technology, at Cambridge, Mass., in 1980, in partial fulfillment of the requirements for the degree of Master of Science.
12. Malhotra, A. K., and Penzien, J., "Nondeterministic Analysis of Offshore Structures," *Journal of the Engineering Mechanics Division*, ASCE, Vol. 96, No. EM6, Dec., 1970, pp. 985–1003.
13. Mes, M. J., "Why Some Structures Jerk in Stormy Seas," *Journal of Ocean Resources Engineering*, Sept., 1977, pp. 24–33.
14. Moan, T., Haver, S., and Vinje, T., "Stochastic Dynamic Response Analysis of Offshore Platforms," *Proceedings of the Offshore Technology Conference*, Paper No. 2407, 1975.
15. Moe, G., and Verley, R. L. P., "An Investigation into the Hydrodynamic Damping of Cylinders Oscillated in Steady Currents of Various Velocities," *Report of the River and Harbor Laboratory*, Norwegian Institute of Technology, June, 1978.
16. Moe, G., and Verley, R. L. P., "Hydrodynamic Damping of Offshore Structures in Waves and Currents," *Proceedings of the Offshore Technology Conference*, Paper No. 3798, 1980.
17. Morison, J. R., O'Brien, M. P., Johnson, J. W., and Schaff, S. A., "The Force Exerted by Surface Waves on Piles," *Petroleum Transactions*, American Institute of Mining Engineers, Vol. 189, 1950, pp. 149–154.
18. Oppenheim, A. V., and Schafer, R. W., *Digital Signal Processing*, Prentice-Hall, Inc., Englewood Cliffs, N.J., 1975.
19. *Proceedings of the Third International Ship Structures Congress*, Oslo, Norway, Sept., 1967.
20. Sarpkaya, T., "Vortex Shedding and Resistance in Harmonic Flow About Smooth and Rough Circular Cylinders at High Reynolds Numbers," *Technical*

Report No. NPS-59SL76021, Naval Postgraduate School, Monterey, Calif., Feb., 1976.
21. Sarpkaya, T., "Vortex Shedding and Resistance in Harmonic Flow about Smooth and Rough Circular Cylinders," *Proceedings of the First International Conference on the Behavior of Offshore Structures*, Vol. 1, 1976, pp. 220–235.
22. Sarpkaya, T., and Isaacson, M., *Mechanics of Wave Forces on Offshore Structures*, Von Nostrand Reinhold, New York, N.Y., 1981.
23. Sarpkaya, T., Collins, N. J., and Evans, S. R., "Wave Forces on Rough-Walled Cylinders at High Reynolds Numbers," *Proceedings of the Offshore Technology Conference*, Paper No. 2901, 1977.
24. Shyam Sunder, S., and Connor, J. J., "Sensitivity Analyses for Steel Jacket Offshore Platforms," *Journal of Applied Ocean Research*, Vol. 3, No. 1, 1981, pp. 13–26.
25. Wu, S. C., and Tung, C. C., "Random Response of Offshore Structures to Wave and Current Forces," *Sea Grant Publication No. UNC-SG-75-22*, Department of Civil Engineering, North Carolina State University, Sept., 1975.

APPENDIX II.—NOTATION

The following symbols are used in this paper:

C = viscous damping matrix;
C_D = hydrodynamic drag force coefficient;
$C_{D\dot{u}}$ = drag coefficient for structural oscillation;
C_{Dv} = drag coefficient for fluid oscillation;
C_M = hydrodynamic inertia force coefficient;
$C_{M\dot{u}}$ = inertia coefficient for structural oscillation;
C_{Mv} = inertia coefficient for fluid oscillation;
D = cylinder diameter;
f = hydrodynamic force per unit length;
f_D = hydrodynamic drag force per unit length;
$\underset{\sim}{F}$ = force vector;
H_s = significant wave height;
k = mean height of surface roughness;
$\underset{\sim}{K}$ = stiffness matrix;
K-C = Keulegan-Carpenter number;
K-C_F = Keulegan-Carpenter number in the far field;
K-C_N = Keulegan-Carpenter number of the near field;
$\underset{\sim}{M}$ = structural mass matrix;
$\underset{\sim}{M}_a$ = added mass matrix;
$\dot{r}$ = relative velocity;
$\dot{r}_o$ = relative velocity amplitude;
R = Reynolds number;
R_F = Reynolds number in the far field;
R_N = Reynolds number in the near field;
T = period of wave oscillation;
T_o = period of cylinder oscillation;
$T_{\dot{r}}$ = average zero-crossing period of relative velocity;
T_s = period of vortex shedding;
$T_{\dot{u}}$ = average zero-crossing period of structural response velocity;
T_v = average zero-crossing period of fluid velocity;
T_z = average zero-crossing period of wave surface elevation;

$\dot{u}$ = structural response velocity;
$\ddot{u}$ = structural response acceleration;
$\underset{\sim}{U}$ = structural response displacement vector;
$\dot{U}_o$ = structural response velocity amplitude;
$\underset{\sim}{\dot{U}}$ = structural response velocity vector;
$\underset{\sim}{\ddot{U}}$ = structural response acceleration vector;
v = fluid velocity;
$\dot{v}$ = fluid acceleration;
V_o = fluid velocity amplitude;
V_R = reduced velocity;
α = artificial damping fraction;
ν = kinematic viscosity of fluid;
ρ = fluid density;
σ_r = r.m.s. relative velocity;
$\sigma_{\dot{u}}$ = r.m.s. structural response velocity; and
σ_v = r.m.s. fluid velocity.